

# 3D printing and its applications in spectroelectrochemistry

Mateus V. Pereira<sup>a</sup>, Evandro Datti<sup>a</sup>, Gabriel R. Alvarenga<sup>a</sup>, Bruno C. Janegitz<sup>b</sup>, J.A. Bonacin<sup>a,\*</sup>

<sup>a</sup>Institute of Chemistry, University of Campinas, 13083-859, Campinas, Sao ~ Paulo, Brazil

<sup>b</sup>Department of Nature Science, Mathematics and Education, Federal University of Sao ~ Carlos (UFSCar), 13600-970, Araras, Sao ~ Paulo, Brazil

## Abstract

The analytical tools have given not only chemistry but science as a whole, new horizons when it comes to the comprehension of chemical phenomena. With precise information, new possibilities emerged in the identification and characterization of novel compounds and advances in several areas of chemistry. In this context, spectroelectrochemistry (*SEC*) combines complementary tools to that the electrochemistry techniques drive the reactions and spectroscopic methods are focused on species analysis. Thus, this strategy provides a way to monitor what is happening *in situ* or *in operando*, making it a powerful tool for the identification of intermediates of reaction, mechanistic, kinetic studies, and even quantitative analysis. However, *SEC* comes with a somewhat inconvenient drawback: even though it has been rising in popularity, setting up the *SEC* cells might be complicated for newcomers. On the other hand, 3D printing becomes interesting and, at the same time, incredibly effective technology for the user to create customized *SEC* cells to support any necessity. In this review, we will go over the importance of 3D printing in the design and use of spectroelectrochemical cells.

Keywords: Spectroelectrochemistry; 3D printing; Additive Manufacturing; Printed *SEC* Cell

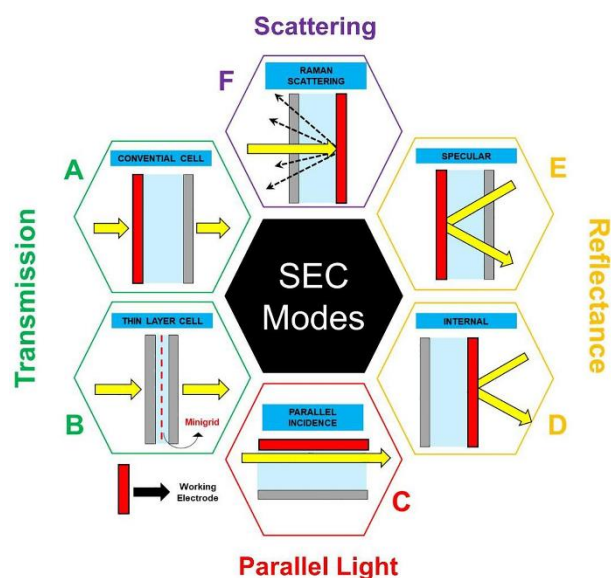
## 35 1. Spectroelectrochemistry as a tool for deep investigation in chemistry

36

37 Chemical information is the key to understand the processes involved in  
38 electrochemistry experiments. Under certain conditions, electrochemical techniques alone are  
39 limited in terms of information and in some cases do not allow a full understanding of the  
40 chemical phenomena behind the electrochemical processes. For this reason, the combination of  
41 electrochemical techniques with spectroscopic analysis is called spectroelectrochemistry (*SEC*)  
42 and it allows scientists to observe the details and changes during the chemical transformations  
43 and contribute to a deep comprehension of the electrochemical interfacial  
44 processes [\[1\]](#), [\[2\]](#), [\[3\]](#), [\[4\]](#).

45 Spectroelectrochemistry is also known as the hyphenation of electrochemistry and  
46 spectroscopy techniques, in other words, an electrochemical reaction (oxidation or reduction)  
47 occurs and it is monitored by spectroscopic methods. Although these are fundamentally  
48 different methodologies, this concept had been developed in the scientific community since the  
49 first optically transparent electrodes (OpTEs) were developed [\[5\]](#). In this setup, the light can  
50 cross the system without any interference and therefore can bring reliable information about the  
51 electrochemical processes on the interface of the electrodes [\[2\]](#), [\[5\]](#), [\[6\]](#).

52 The OpTEs are made of a very thin layer of a conductive material such as Au, Pt,  
53  $\text{In}_2\text{O}_3:\text{SnO}_2$  (ITO – indium tin oxide), or  $\text{SnO}_2:\text{F}$  (FTO – fluorine-doped tin oxide) and they are  
54 promptly within the wide array of possibilities for *SEC*. The proposition consists of what is now  
55 called a thin layer *SEC* under a semi-infinite diffusion regime, which there is a thin layer of the  
56 solution surrounding the electrode, and the optical beam of light directly passes through a  
57 conventional cell [\[6\]](#), a scheme can be found in [Fig. 1 A](#). Later, a new type of OpTE was  
58 introduced and it is currently known as mini-grid working electrodes. These electrodes consist  
59 of a thin plate of metal with small orifices transparent to light in a solution thickness of less  
60 than 0.2 mm (see the scheme in [Fig. 1 B](#)). Mini-grid working electrodes are less susceptible to  
61 artifacts due to the absence of film on their surface [\[2\]](#). They have surface properties like the  
62 bulk Au and present a low internal ohmic resistance. These characteristics contribute to  
63 reproducible measurements for current spectroelectrochemical studies.



64

65 **Fig. 1.** Overview of the spectrochemistry modes. Minigrid: minigrid working electrode.

66

67

68 *SEC* brings countless tools of analysis and allows us to study compounds with low molar  
 69 absorptivity, for example. In this context, a thin layer cell would not be adequate because even  
 70 in high concentrations absorption spectra cannot be measured. The introduction of the long  
 71 optical path length spectroelectrochemical cell solves this problem, since the light beam runs  
 72 parallel to the working electrode in the electrode/solution interface ([Fig. 1 C](#)) [7], [8]. Also, it  
 73 brings the advantage of using any kind of electrode and sensitivity can be modulated according  
 74 to the optical path. The limitations of this technique are the working regime under static  
 conditions, electrolysis time, and the dynamic of superficial adsorption.

75

76 In Raman spectroscopy, the inelastic scattering of incident light over a sample is used  
 77 to get vibrational information about the samples and help to monitor the presence of functional  
 78 groups or surface modification, for example. On the other hand, the combination of Raman  
 79 spectroscopy with electrochemistry experiments allows us to go further and study specific  
 80 mechanisms of reactions and to follow chemical transformations [9]. The  
 81 spectroelectrochemistry Raman enables the use of incident and collection modes with  
 82 backscattering ( $180^\circ$ ), ATR mode, and Raman confocal microscopy. Each mode has vantages  
 83 and disadvantages that can be found in the literature. In addition to conventional Raman is  
 84 possible to perform experiments in resonance regime (Resonance Raman spectroscopy) or  
 85 probing surface through Surface-enhanced Raman spectroscopy (SERS) [10]. A schematic  
 view of the idea of the spectroelectrochemistry Raman is demonstrated in [Fig. 1F](#).

86

87 Although the previously mentioned techniques widely cover the *SEC* analysis, the  
 reflectance modes are essential to complete the set of *SEC* techniques. In specular mode (see

88 scheme in [Fig. 1 E](#)), the light is incident on the reflective surface where it is partly absorbed  
89 and reflected. In specular reflection conditions, the reflectance depends on the angle of  
90 incidence of the source of light [\[11\]](#), [\[12\]](#). Because of this, light can be considered anisotropic  
91 and polarized. On the other hand, the diffuse reflectance is isotropic and emerges from a rough  
92 surface [\[6\]](#), [\[7\]](#). The most common, but not exclusive, application of these techniques is related  
93 to the studies of chemically modified electrodes.

94 The techniques of reflectance are very efficient for spectroscopic analysis but for use  
95 in *SEC*, there are limitations because they request high-concentration solutions or thick films.  
96 To solve this problem the attenuated total reflection (ATR) is an important option. This kind of  
97 internal reflectance spectroscopy (see scheme in [Fig. 1D](#)), for example, allows analysis in thin  
98 films through the interaction of the evanescent wave with the sample. A complete description  
99 of the ATR technique can be easily found in textbooks [\[13\]](#) and the important point for *SEC* is  
100 that the sample must be in contact with the ATR material, usually germanium or OpTE.

101 As seen above, the combination of both spectroscopy and electrochemistry opens many  
102 doors when it comes to applications to understand electrochemical or interfacial processes. The  
103 most noteworthy characteristics are the *in situ* monitoring of a plethora of electrochemical  
104 systems that would be otherwise too difficult to evaluate and, at the same time, gain a deeper  
105 understanding of mechanisms or their kinetic properties [\[14\]](#), [\[15\]](#), [\[16\]](#), [\[17\]](#), [\[18\]](#), [\[19\]](#).

106 One of the biggest challenges in *SEC* is the cell design for *SEC* given that, theoretically,  
107 any spectroelectrochemical method can be carried out as long as the electrochemical cell can  
108 satisfy the requirements of the spectroscopic technique being used. In this context, our goal in  
109 this review is to focus on the fact that the cells can be customized in a myriad of ways to fulfill  
110 their role using 3D printing [\[20\]](#). In this sense, additive manufacturing gives the scientist  
111 freedom of design to print components, pieces, and even electrodes. In addition, the process is  
112 easy to handle, has low cost, and is an incredibly efficient alternative. Given this scenario, we  
113 would like to call attention to this subject as a great opportunity for the popularization of  
114 spectroelectrochemistry.

115

## 116 **2. How can 3D printing assist us in spectroelectrochemistry measurements?**

117

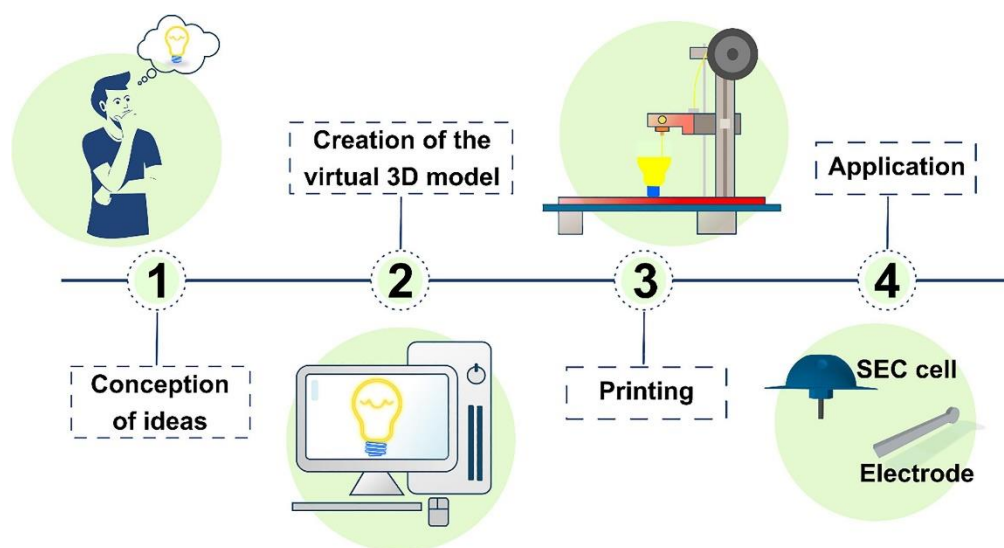
118 Due to recent technological advances and the popularization of additive manufacturing,  
119 3D printing has increasingly gained space in our laboratory routines, which caused the  
120 decentralization of this tool and the modernization of some daily activities [\[14\]](#), [\[16\]](#). An  
121 important area that has benefited from the use of 3D printing is chemistry because its use in the

122 laboratory has enabled the optimization and/or development of parts, supports, and accessories  
123 that can be employed in chemical analysis or monitoring of reactions. Thus, the time and costs  
124 involved in the production of specific parts are strongly reduced [14], [21], [22]. As a  
125 consequence, 3D printing has permeated different areas and many applications are observed in  
126 fields such as energy (both for conversion and storage) [23], [24], adsorption [25], microfluidic  
127 devices [26], and the manufacture of electrodes (to use as sensors and biosensors) [27], for  
128 example.

129 In spectroscopic analysis, 3D printing has been a great tool for creating components and  
130 even equipment. In addition, 3D printing presents itself as a good quality tool with free design  
131 and it is recommended to replace conventional components due to the low cost of  
132 prototyping [28]. This reveals to us the potentiality of the application of this technique and its  
133 versatility in solving problems.

134 3D printing has also been widely used in electrochemistry. This is due to the ease of  
135 building complex systems, which ultimately contributes to price reduction, presenting great  
136 versatility [14], [29], [30]. In this same perspective, the manufacturing of 3D printed electrodes  
137 has been widely developed and with the most diverse applications, among which we can  
138 mention sensors, biosensors, and energy [27], [31]. Among the 3D Printing processes (Fig. 2),  
139 Fused Deposition Modeling (FDM) is the most used for manufacturing these electrodes, due to  
140 its good accessibility, low cost, and ease of operation [27], [32], [33].

141



142

143 **Fig. 2.** Steps in the 3D printing process. 1) The first step is marked by the conception of ideas;  
144 2) The next step is related to the creation of the virtual 3D model of the part; 3) This step is  
145 characterized by the 3D printing of the part that was designed; 4) The last step concerns the  
146 numerous possibilities that exist in the use of 3D printing.

147

148           Among these features, we believe that 3D printing appears as a tool that makes it  
149 possible to assemble personalized *SEC* that can be designed to use different or non-commercial  
150 instruments (i. e. synchrotron laboratories). Another advantage that can be considered is the  
151 freedom during the creation of the cell by the software, providing the conception of alternative  
152 cells to meet the demands. In addition, it allows the analyst to choose the material that will be  
153 used for printing the cell so that there is no interference during the analysis (for example, a  
154 material that is resistant to basic pH can be chosen). Another interesting aspect is that the cell  
155 can be designed in such a way that the volume of sample used during the analysis is  
156 reduced [\[34\]](#).

157           Despite the positive points of the use of 3D printing in the manufacture of spectroscopic,  
158 electrochemical, or spectroelectrochemical cells, it is worth mentioning that there are some  
159 limitations regarding its use. One of these limitations concerns the choice of the 3D printing  
160 technique used. In general, some techniques present better performance than others, mainly  
161 about the finishing of the object or the richness of details, it is up to the user to look for the best  
162 option to meet their needs. Another limitation imposed by the use of this tool is related to the  
163 degree of knowledge, on the part of the user, in the use of software to create three-dimensional  
164 objects. Thus, the analyst should seek knowledge to use these tools or be supported by someone  
165 who has the minimum knowledge to operate.

166

### 167 **3. Applications of 3D printing in spectroelectrochemistry**

168

169           This section presents the main applications and uses of 3D printing to support  
170 experiments involving UV/Vis spectroelectrochemistry (UV/Vis-*SEC*), infrared  
171 spectroelectrochemistry (IR-*SEC*), Raman spectroelectrochemistry (Raman-*SEC*), and XAS  
172 (*X-ray absorption spectroscopy*) spectroelectrochemistry, highlighting some examples found  
173 in the literature.

174

#### 175 *3.1. 3D printing for UV/Vis spectroelectrochemistry (UV/Vis-SEC)*

176

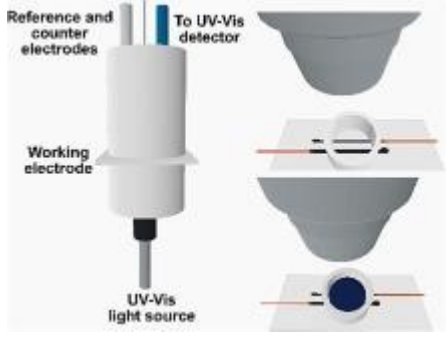
177           Regarding the application of 3D printing in UV/Vis spectroelectrochemistry, an  
178 interesting example is found in the work published by Symes et al. [35]. where a reactionware  
179 was printed and used as an electrochemical cell to monitor the reaction, as can be seen in Table  
180 1. The cell was assembled by Ag/AgCl reference electrode, a Pt wire counter electrode, which

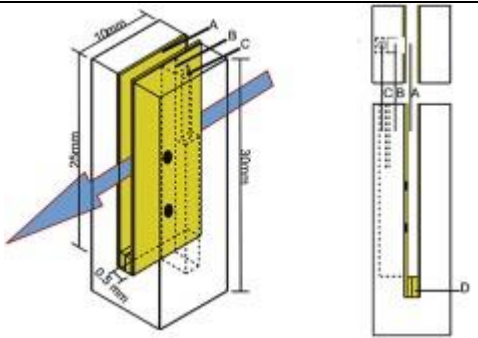
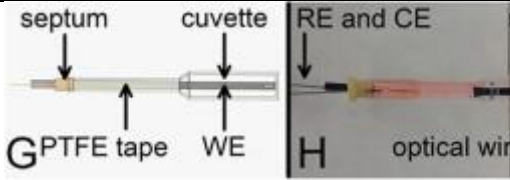
181 were placed into the cited solution, and the ITO slide was used as the working electrode. It has  
 182 been observed a color change in the solution from yellow to slightly blue at  $-0.2$  V, which is  
 183 related to the formation of reduced polyoxomolybdates. To monitor this color change in situ, a  
 184 fiber-optic cable was put through one of the printed holes located at the top of the reactionware  
 185 and then connected to the UV/Vis spectrophotometer. A Hg arc lamp was used to provide the  
 186 input light source in a way that the sample was irradiated from below, allowing the acquisition  
 187 of the UV/Vis spectra. UV/Vis spectrum was then acquired during the electrochemical and  
 188 showed the appearance of a new absorbance peak at around 750 nm associated with a slight  
 189 blue color. Therefore, this study demonstrated that the aforementioned 3D-printed reactionware  
 190 was suitable for spectroelectrochemical analyses [35].

191

192 **Table 1.** Overview of the 3D printed UV/Vis spectroelectrochemistry cell.

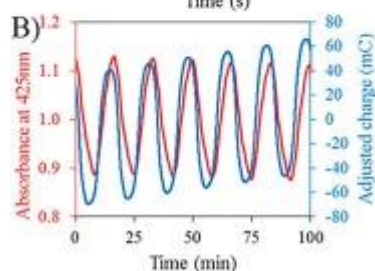
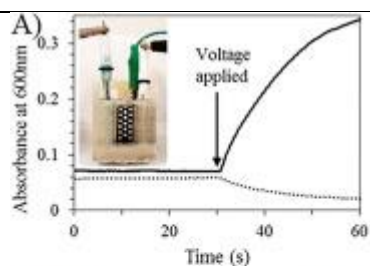
193

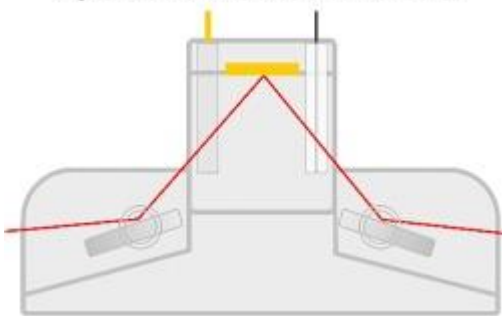
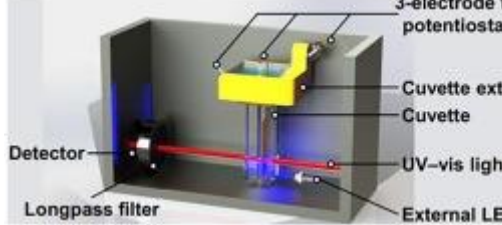
<b>SEC Cell (Technique)</b>	<b>Application</b>	<b>Main feature</b>	<b>Ref.</b>
 <p data-bbox="236 1355 750 1444">Figure was drawn based on information from reference [35].</p>	<p data-bbox="766 1003 1002 1758">The device was used to monitor the color change in situ of the phosphomolybdic acid (PMA) solution in 0.1 M H<sub>2</sub>SO<sub>4</sub>, which is associated with the generation of polyoxomolybdates from the reduction of this compound.</p>	<p data-bbox="1018 1003 1254 2027">Reactionware was printed using a robust and quick-curing acetoxysilicone polymer. The light from the Hg arc lamp passes through the solution contained in this apparatus from below to the UV/Vis detector located at the top of it, allowing the detection of the polyoxomolybda</p>	<p data-bbox="1270 1003 1422 1041"><a href="#">[35]</a>, <a href="#">[40]</a></p>

		tes derived from the reduction of PMA.	
 <p>Reprinted with permission from ref. [34]. © 2013 Elsevier B.V. All rights reserved.</p>	<p>The cell was used to determine the reduction midpoint potential of Safranin O, protein HH, and horse heart cytochrome. Absorbance spectra of the samples were taken between each potential step for building both a kinetic profile and Nernst curve data with a unique titration.</p>	<p>This 3D printed SEC was placed into a standard cuvette, allowing fast spectroelectrochemical titrations of protein or small molecules. Its design maximizes the ratio of the WE surface area to the solution volume while keeping the full path length of the cuvette. A similar system can be used in spectroelectrochemistry experiments related to redox-responsive self-assembled monolayers [41].</p>	<p>[34], [41]</p>
	<p>SEC cell fabricated to monitor three-</p>	<p>In this cell, 3D printed electrode made of</p>	<p>[36]</p>



<p>Reprinted with permission from ref. [36]. © 2019 Elsevier B.V. All rights reserved.</p>	<p>wavelength values during the reduction and re-oxidation of the [Ru(acac)<sub>3</sub>]. Using for investigation of the product formation and the reactant depletion.</p>	<p>composites of PLA and CNT has an optical window (quartz cuvette), which allowed the acquisition of UV/Vis absorbance spectra during the cyclic voltammetric reduction and re-oxidation of [Ru(acac)<sub>3</sub>].</p>	
<p>Reprinted with permission from ref. [37]. Copyright © 2019, American Chemical Society</p>	<p>UV/Vis <i>SEC</i> used to monitor changes in pH during bulk electrolysis.</p>	<p>The working electrode is porous and printed from the conductive filament of PLA. This kind of 3D-printed electrode must be activated to remove the insulating PLA from the surficial layer. This process improves the electrochemical activity of</p>	<p>[37]</p>



		printed electrodes.	
<p style="text-align: center;"><b>Spectroelectrochemical cell</b></p>  <p>Drawn based on information from ref. <a href="#">[38]</a>.</p>	<p>This device was applied to investigate <i>in situ</i> the Prussian blue (PB) growth at the homemade platinum disc working electrode surface.</p>	<p><i>SEC</i> cell manufactured with black color PETG filament and inside it a quartz window was placed to interact between the radiation and electrode surface. Continuous absorbance measurements were carried out at 700 nm, thus monitoring <i>in situ</i> the PB growth.</p>	<p><a href="#">[38]</a></p>
 <p>Reprinted with permission from ref. <a href="#">[39]</a> Copyright © 2021 Wiley-VCH GmbH.</p>	<p>Printed setup for UV/Vis spectroscopy studies of ZnFe<sub>2</sub>O<sub>4</sub> water oxidation intermediates.</p>	<p>The printed setup can be used for UV/Vis spectroelectrochemistry to understand the interfacial reaction and intermediates of the ZnFe<sub>2</sub>O<sub>4</sub> in water oxidation</p>	<p><a href="#">[39]</a>, <a href="#">[42]</a></p>

195 The work carried out by Brisendine *et al.* [34] demonstrated the application of 3D  
196 printing technology to make a microchannel that can be inserted inside of standard cuvettes  
197 ( $1\text{ cm}^2$ ) used in conventional spectrometers in transmission mode, in which the cell design is  
198 depicted in [Table 1](#). The electron transfer kinetics was measured by monitoring the reduction  
199 and oxidation of the potassium ferricyanide. Moreover, protein titrations were made using a  
200 small molecule mediator mixture responsible for mediating electron transfer in the  $-500$   
201 to  $+300\text{ mV}$  range. Complete visible spectra of the samples were taken between each potential  
202 step for building both a kinetic profile and Nernst curve data with a unique titration. This  
203 spectroelectrochemical cell was employed to track the safranin O reduction and oxidation at  
204  $522\text{ nm}$  and the potentiometric titration of this compound.

205 Vaněčková *et al.* have reported the utilization of FDM based 3D printing to produce  
206 electrodes from composites of polylactic acid (PLA) as the binder and carbon nanotubes (CNT)  
207 as the conductive filler. These electrodes were designed to have an optical window, which  
208 enabled them to be used in UV/Vis absorption spectroscopic to detect the electrogenerated  
209 reaction products [36].

210 The goal was then to develop electrochemically active electrodes from PLA/CNT  
211 composite filament for spectroelectrochemical experiments. Besides, since the authors  
212 embedded an optical window on these electrodes, they were employed to carry out UV/Vis  
213 absorption spectroelectrochemical measurements. It is also worth mentioning that this work  
214 was the first reported application of 3D printed electrodes in UV/Vis spectroelectrochemistry.  
215 Such electrodes for UV/Vis spectroelectrochemistry experiments presented a cuboid shape with  
216 dimensions of  $0.75\text{ mm} \times 3.4\text{ mm} \times 110.0\text{ mm}$  and involved a rectangular ( $0.8\text{ mm} \times 4.0\text{ mm}$ )  
217 optical window placed at one end and they were manufactured in batches of five pieces. The  
218 assembled *SEC* cell can be seen in [Table 1](#). Spectroelectrochemical experiments were carried  
219 out in the cyclic voltammetry regime and UV/Vis absorbance spectra were obtained in time  
220 intervals of  $20\text{ s}$ , this condition is necessary for the chemical system to reach equilibrium before  
221 the experiment.

222 In addition, they compared the electrochemical response of 3D printed PLA-CNT  
223 electrodes to the filament not processed by 3D printing. In this scenario, 3D printing of the  
224 filament decreased the values of the separation of cathodic and anodic faradaic maximum,  
225 pointing out that the intrinsic kinetic barrier is considerably reduced. The developed electrodes  
226 were described as fast and cheap to produce because the PLA-CNT composite filament used to  
227 manufacture one 3D printed electrode just cost  $0.04\text{ USD}$  and the fabrication procedure took  
228 only  $6\text{ min}$ . The described experiment was useful to confirm that  $[\text{Ru}(\text{acac})_3]$  used as an

229 electroactive probe reversibly transfers electrons at the interface of the 3D printed PLA-CNT  
230 electrode and the aqueous electrolyte. Besides, the activated 3D printed electrodes presented  
231 electron transfer characteristics similar to those obtained for electrodes manufactured from  
232 conventional carbon-based materials.

233 Wirth *et al.* have described the use of 3D printed electrodes through the FDM technique  
234 for UV/Vis spectroelectrochemistry [37]. The working electrodes were obtained from the  
235 conductive filament of PLA. An important point for this kind of printed electrode is the  
236 introduction of the activation process, which is the removal of the insulating PLA from the  
237 surficial layer. This process improves the electrochemical activity of printed electrodes. The  
238 setup presented in this work allows the use of a three-component electrochemical cell where  
239 the working electrode is printed and spectroscopically monitored by a conventional UV/Vis  
240 spectrophotometer.

241 Print electrodes remove limitations of the design and introduce the numberless  
242 possibilities of setup and applications. For example, the authors focused on their studies to  
243 observe the pH change during the water electrolysis using a UV/Vis-SEC with a printed  
244 working electrode.

245 Another application of 3D printing in UV/Vis spectroelectrochemistry is found in an  
246 interesting paper written by da Silva Junior *et al.* in which the authors described in detail the  
247 fabrication of 3D printed SEC for *in situ* UV/Vis measurements [38]. The electrochemical  
248 setup was made using a system composed of three electrodes, in which the working electrode  
249 was a homemade platinum disc electrode, an Ag/AgCl as a reference electrode, and a platinum  
250 wire as an auxiliary electrode.

251 The SEC cell, all accessories, and sample holders were manufactured using black color  
252 PETG (polyethylene terephthalate glycol) filament to substitute the original spectrometers, as  
253 represented in [Table 1](#). Inside the cell, the sample surface of the working electrode was  
254 vertically disposed and a quartz window was placed to interact between the radiation and  
255 electrode surface. Besides, 18 h were approximately spent to print this UV/Vis SEC with an  
256 estimated cost of about 15 USD.

257 To evaluate the performance of this SEC cell, electrodeposition of Prussian Blue film in  
258 the working electrode was made by applying a potential of + 0,3 V against the reference  
259 electrode with the use of a potentiostat for 200 s, allowing the reaction between potassium  
260 ferricyanide and ferric chloride. Meanwhile, the continuous absorbance measurements were  
261 carried out at 700 nm, which is the intervalence charge-transfer band for the Prussian Blue (PB),  
262 allowing the *in situ* observation of the PB film growth. This 3D printed spectroelectrochemical

263 cell demonstrated the capacity of the 3D printing technology to manufacture bespoke  
264 accessories for spectroelectrochemistry analysis [38].

265 The interesting printed setup presented by Yongpeng Liu and collaborators [39] can be  
266 used for spectroelectrochemistry-UV/Vis to understand the interfacial reaction and  
267 intermediates produced during the photochemical water oxidation by  $ZnFe_2O_4$ . The  
268 comprehension of the interfacial processes and recombination can be used to improve the  
269 properties of the catalyst;

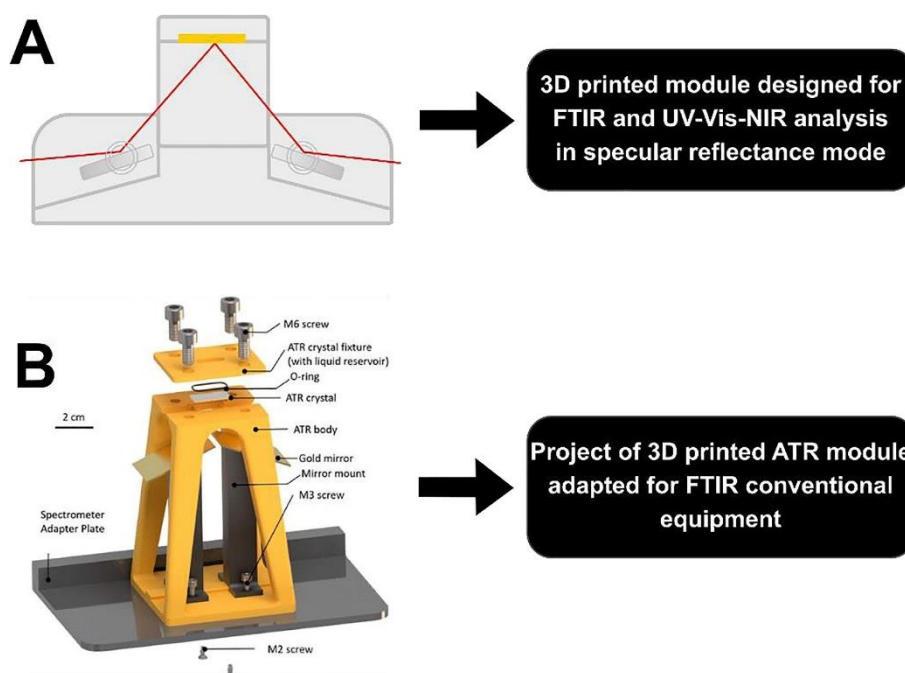
270

### 271 3.2. 3D printing infrared spectroelectrochemistry

272

273 The 3D printed modules presented by Silva Junior et al. and Baumgartner et al. are  
274 objects used in conventional spectroscopic analysis. Fig. 3A shows the impression of a specular  
275 reflectance module for ex-situ experiments. The support was designed to couple two mirrors  
276 and it can be used in UV/Vis-NIR and FT-IR analysis. Another interesting project is presented  
277 in Fig. 3B where the attenuated total reflection module was designed and printed in a 3D printer  
278 - FDM. This object was projected for ATR-IR analysis and can be adapted for different  
279 equipment. Both projects have low-cost, fast production and might be adjusted for any setup.  
280 Although these proposals do not contemplate the use of FT-IR SEC, the coupling of the original  
281 projects with an electrochemical cell might be possible.

282



283

284 Fig. 3. A) 3D printed accessory for spectroscopic analysis (FTIR) by specular reflectance, a  
 285 figure drawn based on information from reference [38]; B) 3D printed ATR module adapted  
 286 for FT-IR analysis Copyright © 2020, American Chemical Society.

287

### 288 3.3. 3D printing for Raman spectroelectrochemistry (Raman-SEC)


289


290 3D printing technology's use for manufacturing a spectroelectrochemical cell and a  
 291 working electrode to carry out *in situ* Raman measurements was demonstrated in the paper  
 292 written by dos Santos *et al.* [9]. Raman spectroelectrochemistry has some limitations that are  
 293 related to the elevated cost and the complexity of the commercial spectroelectrochemical cells  
 294 used in this technique. However, such drawbacks can be circumvented by the introduction of  
 295 3D printing technologies, which they offer an alternative to designing such a system in a much  
 296 cheaper, simpler, and more versatile way in a short period. In this context, the authors have  
 297 shown the fabrication of a dome-shaped SEC using acrylonitrile – butadiene – styrene (ABS)  
 298 filament to fit the Raman objective lens in the center hole of the spectroelectrochemical cell  
 299 above the working electrode's surface and two other holes were added to fit the reference  
 300 electrode (Ag/AgCl, 3 mol.L<sup>-1</sup>) and Pt counter electrode, as it is depicted in Table 2. Apart from  
 301 that, the working electrode with a screw shape was printed using a conductive graphene-based  
 302 PLA filament. Both the SEC and the 3D-printed electrode were printed within 3.5 h with a very  
 303 low cost of materials used, which was estimated at less than 2 USD [9].

304

305 **Table 2.** Overview of the SEC – Raman cell.

306

SEC Cell (Technique)	Application	Main feature	Ref.
 <p data-bbox="244 1814 829 1904">Reprinted with permission from ref. [9]. Copyright 2019 American Chemical Society.</p>	<p data-bbox="869 1552 1098 2027">It was used to study structural changes in Prussian Blue during electrochemical measurements. <i>In situ</i> Raman spectra of this</p>	<p data-bbox="1129 1552 1334 2027">This SEC cell was printed using ABS filament in a dome shape in order to fit Raman objective lens in the center</p>	<p data-bbox="1366 1552 1417 1585"><a href="#">[9]</a></p>

	<p>compound were acquired to investigate the shifts in the frequency of the CN stretching band as a function of the applied potential.</p>	<p>hole of the cell, enabling the obtainment of Raman spectra while the electrochemical measurements were made. In addition, the working electrode was also printed in a screw shape and after modified with Prussian blue.</p>	
 <p>Figure drawn based on information from ref. <a href="#">[38]</a>.</p>	<p>It was applied to track the Prussian blue growth film process. Raman spectra were obtained continuously, allowing the characterization of the PB forms. Moreover, this system was also used to real-time accompany the electrochemical conversion of PB film into the</p>	<p>It was made using black color PETG filament and its design enabled it to receive three or more electrodes to perform dynamic flux measurements. Raman spectra were obtained using 633 nm laser every 20 s during the reaction</p>	<p><a href="#">[38]</a></p>

	Prussian white and Berlin Green.	between potassium ferricyanide and ferric chloride in order to monitor the presence of CN bands.	
--	----------------------------------	--	--

307

308           These facts emphasize the advantages of using additive manufacturing, its simplicity,  
309 fast prototyping capabilities, and the possibility of designing any type of device with the desired  
310 shape and dimension make it suitable for a wide variety of applications, such as the monitoring  
311 of reactions *in situ* or *modus operandi*. This system was then employed to study structural  
312 changes in Prussian Blue (PB) during electrochemical measurements. *In situ* Raman spectra of  
313 this compound were acquired in the electrode potential range from -0,4 to + 1.2 V vs Ag/AgCl,  
314 which enabled the investigation of the shifts in the frequency of the CN stretching band as a  
315 function of the applied potential. According to the results, the printed electrode proved to be  
316 good support for anchoring the PB particles, besides it showed a comparable electrochemical  
317 behavior to the commercial glassy carbon electrode [9].

318           Another example regarding the application of 3D printing technology in Raman  
319 spectroelectrochemistry can be found in the paper published by da Silva Junior *et al.* mentioned  
320 before [38]. In this work, 3D printed accessories were developed to unite *ex situ* or *in*  
321 *situ* electrochemical and spectroscopic techniques to study dynamic interfacial and surface  
322 phenomena, including the *SEC* for Raman microspectroscopy analysis able to work in flux or  
323 a stationary regime. The design of the cell allowed its use with the available equipment and  
324 compatibility with common commercial electrodes was achieved, besides it involved a simple,  
325 cheap, sustainable, and low-time production process.

326           The spectroelectrochemical cell was made utilizing PETG filament due to its good  
327 chemical and high impact resistance, ease of printing, and outstanding durability. The design  
328 of the printable parts was performed using an online 3D app such as *Tinkercad*<sup>TM</sup> in a way to  
329 obtain the working electrode surface facing upwards, enabling it to receive an array of three or  
330 more electrodes to carry out dynamic flux measurements, as can be visualized in [Table 2](#).



331 The time spent printing the Raman-SEC was about 6 h with an estimated cost of around  
332 15 USD. The performance of this 3D-printed device was evaluated by tracking the Prussian  
333 Blue growth film over the Pt working electrode using 0.1 mol.L<sup>-1</sup> KCl electrolyte. A potential  
334 of + 0.3 V vs Ag/AgCl (3 M KCl) was applied for 200 s to drive the reaction between potassium  
335 ferricyanide and ferric chloride, the Raman-SEC cell was then used to obtain a spectrum in the  
336 wavenumber range from 1600 to 2600 cm<sup>-1</sup> using 633 nm laser every 20 s.

337 This experiment permitted the characterization of the PB forms by the change of CN  
338 stretch bands between 2000 and 2200 cm<sup>-1</sup>. Over again, the possibilities and application depend  
339 on the problem, creativity, and ability to design/print cells for Raman equipment.

340

#### 341 3.4. XAS spectroelectrochemistry (XAS-SEC)

342

343 Fabrication of 3D-printed multi-purpose electrochemical devices for X-ray absorption  
344 spectroscopy (XAS) is well described in the paper written by Achilli *et al.*. It demonstrated the  
345 use of 3D printing for the development of electrochemical cells to be employed in experiments  
346 with *in situ* and *in operando* characteristics using synchrotron radiation, which allows a  
347 detailed investigation of systems in their real working conditions [43].

348 It is worth mentioning that the use of synchrotron radiation as a characterization tool  
349 requires the connection of the beamlines to distinct experimental setup demands, which means  
350 that the creation of a suitable arrangement to control the physicochemical conditions of the  
351 sample is often difficult. In this context, advantages that arise from the use of this technology  
352 to create the mentioned electrochemical devices are underlined, such as the precision of the 3D  
353 printing system, which enables the manufacture of the cells with the required details, making  
354 the combination of synchrotron-based methods with electrochemical techniques viable. It is  
355 reported in this paper the design of two different types of spectroelectrochemical cells for XAS  
356 experiments on photoanodes for photoelectrochemical water splitting [43].

357 Photoanodes studied for water oxidation were composed of the catalytic domain made  
358 of IrOx and hematite. The main objective was to investigate the mechanism and the kinetics of  
359 electrocatalytic reactions. In this case, limits on the illumination by X-rays and UV/Vis light  
360 exist due to the coupling between the hematite and IrOx. In their structure, hematite is deposited  
361 over the FTO substrate which strongly absorbs wavelengths in the range of near-UV, and the  
362 IrOx layer which absorbs in the visible region is placed upon the hematite layer. The aim of  
363 using the X-ray probe in each experiment was to investigate the local electronic changes in the  
364 IrOx overlayer caused by the illumination of hematite and because of the attenuation coefficient

365 of the materials present, XAS investigation was carried out on the side of the IrOx film and in  
 366 fluorescence mode.

367 Given these boundary conditions, the authors developed photo-spectroelectrochemical  
 368 cells for containing the photoanodes, and besides they were designed to have three electrodes,  
 369 a reference electrode, a counter electrode, and the working electrode, which is the photoanode.  
 370 Their design and fabrication made the importance and practicality of 3D printing evident,  
 371 because these devices have small channels and holes, which should ensure the electrical contact  
 372 between the three electrodes by the electrolyte, something extremely hard to be obtained using  
 373 conventional tools or manually.

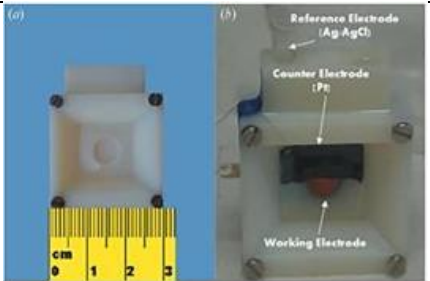
374 These photo-spectroelectrochemical devices should also be resistant to X-rays,  
 375 otherwise, they would suffer from the formation of holes and consequently loss of mass. Thus,  
 376 the application of a 3D printer with the use of photopolymers resin was able to meet all the  
 377 material requirements, being the easiest and fastest way to manufacture efficient photo-  
 378 spectroelectrochemical cells with the necessary details compared to the conventional  
 379 subtractive manufacturing technologies.

380 The two photo-spectroelectrochemical apparatuses demonstrated in this article were  
 381 called cell types A and B (see [Table 3](#)). Both cells were fabricated using a photopolymer-based  
 382 3D printer. Cell type A is composed of two parts linked by screws and bolts and a frontal  
 383 circular window was put in for illumination by UV/Vis and X-ray photons ([Table 3](#)). In the  
 384 working electrode, XAS investigation was carried out in the electrocatalyst IrOx and the  
 385 hematite part of the electrode was illuminated by UV/Vis light.

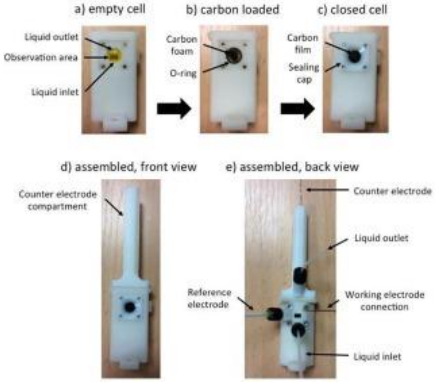
386

387 **Table 3.** Overview of the *SEC* – XAS.

388

<b>SEC Cell (Technique)</b>	<b>Application</b>	<b>Main feature</b>	<b>Ref</b>
 <p>Reprinted with permission from ref. <a href="#">[43]</a>. Copyright 2016,</p>	<p><b>Cell type A</b> was developed to investigate electrodeposited IrOx overlayers in the working electrode. Local electronic changes in this overlayer were</p>	<p><i>SEC</i> cell made of photopolymers resin is composed of two parts and a frontal circular window that allows the illumination by UV/Vis and X-ray photons.</p>	<p><a href="#">[43]</a></p>

<p>International Union of Crystallography.</p>	<p>studied by using the X-ray probe.</p>	<p>XAS investigation was performed in the electrocatalyst IrOx in fluorescence mode while the hematite part of the working electrode was illuminated by UV-vis light.</p>	
<div data-bbox="240 730 683 898" data-label="Image"> </div> <p>Reprinted with permission from ref. [43]. Copyright 2016, International Union of Crystallography</p>	<p><b>Cell type B</b> was fabricated to study photoelectrodeposited IrOx overlayers upon the working electrode. With its use of it, a better understanding of the mechanism and the kinetics related to the photoelectrocatalytic process of water splitting was achieved.</p>	<p>This cell has a circular hole providing a window to the working electrode. Its left side was illuminated by UV/Vis while the right side received X-ray illumination, enabling the study of the different responses of the catalyst under UV/Vis light and dark conditions</p>	<p>[43]</p>
<div data-bbox="240 1442 515 1711" data-label="Image"> </div> <div data-bbox="240 1711 515 1928" data-label="Image"> </div> <p>Reprinted with permission from [44]. Copyright 2021,</p>	<p>X-ray absorption spectra were obtained from copper (II) solutions by using this XAS-SEC cell to show that electrochemical control can enable a repeated analysis of solutions sensitive to photoreduction without</p>	<p>XAS-SEC cell is made of a rigid UV-cured Polymer. A Ag/AgCl reference electrode and porous reticulated vitreous carbon working electrode were employed. The copper solutions were transferred to gas-tight syringes and valves in a</p>	<p>[44]</p>

<p>International Union of Crystallography.</p>	<p>considerable change to the XANES. Open circuit potential was altered in the absence and presence of illumination during the spectra acquisition to evaluate the susceptibility of the sample to oxidation and reduction.</p>	<p>glove box. Afterward, the syringes were connected to the cell, ensuring precise control of the solution flow. It was developed for controlling redox state and photoreduction from solutions of species sensitive to photodamage.</p>	
 <p>Reproduced with permission from ref. [45]. Copyright 2019, International Union of Crystallography.</p>	<p>XAS-SEC cell for time-resolved X-ray absorption spectroelectrochemistry experiments in a homogeneous medium</p>	<p>This printed cell was used in time-resolved X-ray spectroelectrochemistry experiments. The object of this research is to probe transient species produced during the electrochemical experiment. Thus, it is possible to investigate the local and electronic structure of redox-active species in solution through time-resolved X-ray spectroscopy.</p>	<p>[45]</p>

389

390

391

The cell type B was designed with a circular hole in the rectangular cover, providing a window on the working electrode to perform UV/Vis spectroscopy. This cell has also a

392 rectangular-shaped electrolyte chamber which presents an upper slot, making the insertion of  
393 the Pt counter electrode easier, as depicted in [Table 3](#).

394 More importantly, according to the results collected these 3D-printed cells worked. It  
395 was made a comparison between cyclic voltammetry obtained employing a 3D-printed XAS  
396 cell and one obtained using a standard electrochemical cell, in both cases, the cell response was  
397 very similar. With the use of these photo-spectroelectrochemical cells was possible to study the  
398 different responses of the catalyst under UV–Vis light and dark conditions, which resulted in a  
399 better understanding of the mechanism and the kinetics associated with the  
400 photoelectrocatalytic process of water splitting.

401 The paper published by Best *et al.* describes CAD-based design and 3D printed XAS-  
402 SEC cells, as can be seen in [Table 3](#). The work aimed to control the redox state and the  
403 photoreduction of species sensitive to photodamage in solution. This article highlighted the  
404 benefits of coupling CAD design with 3D printing, which allows the accomplishment of more  
405 difficult designs and low-cost units [\[44\]](#).

406 A problem to be overcome during the measuring of X-ray absorption spectra of the first-  
407 row transition metals at the K edge is photoreduction. A possible solution was the development  
408 of methods that enable the acquisition of XAS spectra at energies higher than 4 KeV from small  
409 volumes of solution samples at room temperature under potentiostatic control. Additive  
410 manufacturing guided by CAD packages was used in this work to manufacture highly optimized  
411 3D printed XAS-SEC cells at a low-cost, in which the quality of the data obtained using this  
412 system was demonstrated.

413 Besides, the design of an integrated stepper motor syringe pump was also shown.  
414 Measurements of copper(II) complexes were made to show that electrochemistry together with  
415 flow control can permit repeated analysis of a defined volume of the solution of samples  
416 sensitive to photoreduction without significant change to the X-ray absorption near-edge  
417 structure (XANES). During the data acquisition of the XANES, the open circuit potential (OCP)  
418 was varied in the absence and presence of illumination to evaluate the susceptibility of the  
419 sample to oxidation or reduction during measurement.

420 X-ray absorption spectra of copper solution (2 mM in phosphate buffer under an inert  
421 atmosphere) were acquired using the I20-Scanning wiggler beamline of Diamond Light Source.  
422 Ag/AgCl reference electrode and porous reticulated vitreous carbon working and counter  
423 electrode were used in the XAS spectroelectrochemical cell. Its design was implemented by  
424 employing the open-source software OpenSCAD. Besides, a Connex3 Objet350 3D printer with

425 UV-cured ink and water-soluble support was used to fabricate objects with high geometric  
426 precision appropriate for working with aqueous solutions.

427 In terms of the material used, although the UV-cured polymer is rigid, it's brittle and its  
428 compatibility with non-aqueous solvents is poor. Thus, this 3D printed cell had the limitation  
429 in repeated use due to the material's characteristics, but it is compensated by its low unit cost.  
430 Regarding the electrochemical cell, it had porous reticulated vitreous carbon WE and CE with  
431 Ag/AgCl reference placed close to the WE. Moreover, the space between the electrodes was  
432 filled with glass beads to minimize the mixing of the solution in the WE and CE. A graphite  
433 rod was also used to establish electrical connections to the working and counter electrodes. The  
434 cell was connected to the syringes, in which fine control over the volume and rate of the solution  
435 was made to guarantee a successful cell's operation. XAS-SEC cell was placed into an acrylic  
436 box to decrease air scatter and fix the angle between the incident beam and the surface of the  
437 working electrode positioned at 45°.

438 The authors have reported that the optimization of the flow rate parameters and beam  
439 intensity allows the attainment of high-quality XAS spectra from small solution volumes.  
440 Furthermore, thanks to the advances in 3D printing, and more accessibility to commercial  
441 printing, considerable improvements have been made in the electrochemical performance and  
442 reliability, leading to the minimization of sample volume and XAS spectra with better quality.

443 Another example of XAS-SEC, presented by Khaled Cheaib and collaborators,  
444 describes the design and construction of a spectroelectrochemical cell (transmission mode) for  
445 time-resolved X-ray absorption spectroscopy in the homogeneous medium. This cell allows  
446 studies of the electronic structure and identification of active species or oxidation states in  
447 solution through time-resolved spectroscopy [\[45\]](#).

448

#### 449 **4. Final remarks about using 3D printing in spectroelectrochemistry**

450

451 Additive manufacturing introduces new possibilities to spectroelectrochemistry due to  
452 the low cost and fast prototyping to create spectroelectrochemical cells. Moreover, the freedom  
453 of design allows us to create printed SEC for any type of equipment for spectroscopy analysis  
454 and facilitates the coupling with a potentiostat. In this way, existing equipment can deliver even  
455 more in characterization and understanding of chemical reactions, identification of  
456 intermediates of reaction, mechanistic analysis, kinetic studies, and even quantitative analysis.

457 These features of 3D printing enable the user to manufacture bespoke accessories and  
458 electrodes rapidly to meet the requirements of a given experimental setup, without the need of

459 using expensive materials and drastically reducing the generation of waste during the  
460 fabrication of the *SEC* cell in comparison with the conventional subtractive manufacturing  
461 technologies. The examples cited in section 3 highlighted the advantages of additive  
462 manufacturing, making it possible to create devices able to monitor several reactions *in*  
463 *situ* and *in operando* by coupling spectroscopic and electrochemical techniques.

464 Although 3D printing brings great freedom in the development and creation of objects  
465 that can be used in spectroelectrochemical analyses, some limitations must be considered. One  
466 of the main limitations is related to the type of polymer used during 3D printing, because  
467 depending on the solvent or pH of the medium, the durability of the cell will be affected,  
468 considering the behavior of the polymer against these factors. As has also been reported, it is  
469 sometimes necessary to print more than once of the same cell, to make the experiment  
470 reproducible. However, it is interesting to note that even printing several repeated accessories,  
471 the cost involved in this process is very low, making this path viable.

472 FDM and digital light processing (DLP) are nowadays the main additive manufacturing  
473 techniques used to print *SEC*. The FDM technique uses ABS and PLA as polymeric filaments.  
474 ABS has excellent stability in acid and alkaline conditions but resists organic-based solvents  
475 poorly (either suffers from considerable swelling or outright solubilization), while PLA  
476 struggles with swelling for most solvents except for water and cannot stand very acidic or  
477 alkaline systems. 3D-printed objects from resin with UV cure through the DLP technique  
478 usually are stable in mild acid and alkaline conditions and they are relatively stable in organic  
479 solvents. However, stability can change depending on the type of resin used.

480 Another visible limitation is related to the time established for optimizing the 3D  
481 printing parameters. Optimizing the 3D printing parameters is very important as they will  
482 determine the quality of the print, so in some cases, it takes considerable time. However, once  
483 these parameters are adjusted, they can be saved as soon as the same object is printed, it will  
484 only be necessary to keep the parameters that were established previously as optimal.

485 3D printing is still influenced by the material used and there can be many possibilities.  
486 Certainly, it depends on the richness of details that the object/accessory will have to use  
487 spectroelectrochemical analyses. But in general, among the techniques used, FDM stands out  
488 for its cost, speed, and ease of use. Besides, the use of 3D printing by DLP techniques is  
489 increasing due to the reduced cost observed for UV cure resins and the quality of the final piece.

490 3D printed electrodes can be an alternative to conventional electrodes mainly when  
491 some restriction of size or setup is required. They can also be printed fastly and at a low cost.  
492 Finally, we believe that 3D printing using different techniques can be a turning point in the

493 popularization of spectroelectrochemistry analysis and we acknowledge the huge potential that  
494 3D-printed electrodes have due to their versatility and cost, making them pair incredibly well  
495 with the number of experiments that can be done.

496 Finally, we observe that 3D printing allows freedom for the printing project of an *SEC* to  
497 most of the equipment available in a research lab. Moreover, it would be an unparalleled  
498 opportunity to produce very specific *SEC* to solve relevant problems and a starting point to  
499 popularize spectroelectrochemical techniques.

500

#### 501 **CRedit authorship contribution statement**

502 **Mateus V. Pereira:** Conceptualization, Investigation, Writing – original draft. **Evandro**  
503 **Datti:** Investigation, Writing – original draft. **Gabriel R. Alvarenga:** Investigation, Writing –  
504 original draft. **Bruno C. Janegitz:** Conceptualization, Writing – review & editing. **J.A.**  
505 **Bonacin:** Supervision, Conceptualization, Writing – review & editing.

506

#### 507 **Declaration of Competing Interest**

508

509 The authors declare that they have no known competing financial interests or personal  
510 relationships that could have appeared to influence the work reported in this paper.

511

#### 512 **Acknowledgments**

513

514 The authors are grateful for the financial support of the Brazilian Funding Agencies. This study  
515 was financed in part by the Coordenação de Aperfeiçoamento de Pessoal de Nível Superior -  
516 Brasil (CAPES) - Finance Code 001 and grant# 88887.510506/2020-00, Conselho Nacional de  
517 Desenvolvimento Científico e Tecnológico CNPq (grant# 303338/2019-9 and  
518 grant#308203/2021-6) and Fundação de Amparo à Pesquisa do Estado de São Paulo, FAPESP  
519 (grant#2017/11986-5, grant# 2017/21097-3, grant# 2020/14769-8, grant#2021/05976-2).

520

#### 521 **References**

522

523 [1] W.R. Heineman, spectro-electro-chemistry, *Anal. Chem.* 50 (1978) 390A–402A,  
524 <https://doi.org/10.1021/ac50025a789>.

525 [2] M. Petek, T.E. Neal, R.W. Murray, Application of optically transparent minigrid electrodes  
526 under semiinfinite diffusion conditions, *Anal. Chem.* 43 (8) (1971) 1069–1074.



- 527 [3] H. Toma, K. Araki, Spectroelectrochemical characterization of organic and metalorganic  
528 compounds, *COC* 6 (2002) 21–34, <https://doi.org/10.2174/1385272023374607>.
- 529 [4] W. Kaim, J. Fiedler, Spectroelectrochemistry: the best of two worlds, *Chem. Soc. Rev.* 38  
530 (2009) 3373–3382, <https://doi.org/10.1039/B504286K>.
- 531 [5] T. Kuwana, R.K. Darlington, D.W. Leedy, Electrochemical studies using conducting glass  
532 indicator electrodes, *Anal. Chem.* 36 (10) (1964) 2023–2025.
- 533 [6] W.R. Heineman, Spectroelectrochemistry: the combination of optical and electrochemical  
534 techniques, *J. Chem. Educ.* 60 (1983) 305, <https://doi.org/10.1021/ed060p305>.
- 535 [7] T.E. Keyes, R.J. Forster, Spectroelectrochemistry, in: *Handbook of Electrochemistry*,  
536 Elsevier, 2007, pp. 591–635, <https://doi.org/10.1016/B978-044451958-0.50027-6>.
- 537 [8] J. Lopez-Palacios, A. Colina, A. Heras, V. Ruiz, L. Fuente, Bidimensional  
538 spectroelectrochemistry, *Anal. Chem.* 73 (2001) 2883–2889, <https://doi.org/10.1021/ac0014459>.
- 540 [9] M.F. dos Santos, V. Katic, P.L. dos Santos, B.M. Pires, A.L.B. Formiga, J.A. Bonacin, 3D-  
541 Printed low-cost spectroelectrochemical cell for in situ raman measurements, *Anal. Chem.* 91  
542 (2019) 10386–10389, <https://doi.org/10.1021/acs.analchem.9b01518>.
- 543 [10] Y. Zhai, Z. Zhu, S. Zhou, C. Zhu, S. Dong, Recent advances in spectroelectrochemistry,  
544 *Nanoscale*. 10 (2018) 3089–3111, <https://doi.org/10.1039/C7NR07803J>.
- 545 [11] J.L. Bott-Neto, M.V.F. Rodrigues, M.C. Silva, E.B. Carneiro-Neto, G. Wosiak, J. C.  
546 Mauricio, E.C. Pereira, S.J.A. Figueroa, P.S. Fernández, Versatile spectroelectrochemical cell  
547 for in situ experiments: development, applications, and electrochemical behavior\*\*,  
548 *ChemElectroChem*. 7 (2020) 4306–4313, <https://doi.org/10.1002/celec.202000910>.
- 549 [12] S.A. Carminati, B.L. da Silva, J.L. Bott-Neto, M.A. de Melo, M.T. Galante, P. S. Fern´  
550 andez, C. Longo, J.A. Bonacin, A.F. Nogueira, Hematite nanorods photoanodes decorated by  
551 cobalt hexacyanoferrate: the role of mixed oxidized states on the enhancement of  
552 photoelectrochemical performance, *ACS Appl. Energy Mater.* 3 (10) (2020) 10097–10107.
- 553 [13] D.A. Skoog, F.J. Holler, S.R. Crouch, *Principles of Instrumental Analysis*, Cengage  
554 Learning, 2017 [https://books.google.com.br/books?id=jK\\_FDQAAQBAJ](https://books.google.com.br/books?id=jK_FDQAAQBAJ).
- 555 [14] M.J. Whittingham, R.D. Crapnell, E.J. Rothwell, N.J. Hurst, C.E. Banks, Additive  
556 manufacturing for electrochemical labs: An overview and tutorial note on the production of  
557 cells, electrodes and accessories, *Talanta Open*. 4 (2021), 100051,  
558 <https://doi.org/10.1016/j.talo.2021.100051>.
- 559 [15] S. Rouf, A. Raina, M. Irfan Ul Haq, N. Naveed, S. Jeganmohan, A. Farzana Kichloo, 3D  
560 printed parts and mechanical properties: Influencing parameters, sustainability aspects, global

561 market scenario, challenges and applications, advanced Industrial and engineering polymer,  
562 Research. 5 (3) (2022) 143–158.

563 [16] A.J. Lopes, M.A. Perez, D. Espalin, R.B. Wicker, Comparison of ranking models to  
564 evaluate desktop 3D printers in a growing market, Additive Manufacturing. 35 (2020), 101291,  
565 <https://doi.org/10.1016/j.addma.2020.101291>.

566 [17] O. Abdulhameed, A. Al-Ahmari, W. Ameen, S.H. Mian, Additive manufacturing:  
567 challenges, trends, and applications, Adv. Mech. Eng. 11 (2019), 1687814018822880,  
568 <https://doi.org/10.1177/1687814018822880>.

569 [18] R. Varghese, S. Salvi, P. Sood, J. Karsiya, D. Kumar, 3D printed medicine for the  
570 management of chronic diseases: the road less travelled, Annals of 3D Printed Medicine. 5  
571 (2022), 100043, <https://doi.org/10.1016/j.stlm.2021.100043>.

572 [19] S.A. Khaled, J.C. Burley, M.R. Alexander, J. Yang, C.J. Roberts, 3D printing of fivein-  
573 one dose combination polypill with defined immediate and sustained release profiles, J.  
574 Controlled Release 217 (2015) 308–314, <https://doi.org/10.1016/j.jconrel.2015.09.028>.

575 [20] L. Leon, J.D. Mozo, Designing spectroelectrochemical cells: a review, TrAC Trends  
576 Anal. Chem. 102 (2018) 147–169, <https://doi.org/10.1016/j.trac.2018.02.002>.

577 [21] E.K. Grasse, M.H. Torcasio, A.W. Smith, Teaching UV–Vis spectroscopy with a  
578 3Dprintable smartphone spectrophotometer, J. Chem. Educ. 93 (2016) 146–151,  
579 <https://doi.org/10.1021/acs.jchemed.5b00654>.

580 [22] M. Renner, A. Griesbeck, Think and print: 3D printing of chemical experiments, J. Chem.  
581 Educ. 97 (2020) 3683–3689, <https://doi.org/10.1021/acs.jchemed.0c00416>.

582 [23] M.P. Browne, E. Redondo, M. Pumera, 3D printing for electrochemical energy  
583 applications, Chem. Rev. 120 (2020) 2783–2810, <https://doi.org/10.1021/acs.chemrev.9b00783>.

584 [24] K. Ghosh, S. Ng, C. Iffelsberger, M. Pumera, 2D MoS<sub>2</sub>/carbon/polylactic acid filament  
585 for 3D printing: photo and electrochemical energy conversion and storage, Applied Materials  
586 Today. 26 (2022), 101301, <https://doi.org/10.1016/j.apmt.2021.101301>.

587 [25] D. Wang, T. Zhi, L. Liu, L. Yan, W. Yan, Y. Tang, B. He, L. Hu, C. Jing, G. Jiang, 3D  
588 printing of TiO<sub>2</sub> nano particles containing macrostructures for As(III) removal in water, Sci.  
589 Total Environ. 815 (2022), 152754, <https://doi.org/10.1016/j.scitotenv.2021.152754>.

590 [26] N. Weigel, M.J. Mannel, J. Thiele, Flexible materials for high-resolution 3D printing of  
591 microfluidic devices with integrated droplet size regulation, ACS Appl. Mater. Interfaces. 13  
592 (2021) 31086–31101, <https://doi.org/10.1021/acsami.1c05547>.

593

594 [27] R.M. Cardoso, C. Kalinke, R.G. Rocha, P.L. dos Santos, D.P. Rocha, P.R. Oliveira, B. C.  
595 Janegitz, J.A. Bonacin, E.M. Richter, R.A.A. Munoz, Additive-manufactured (3Dprinted)  
596 electrochemical sensors: a critical review, *Anal. Chim. Acta.* 1118 (2020) 73–91,  
597 <https://doi.org/10.1016/j.aca.2020.03.028>.

598 [28] B. Baumgartner, S. Freitag, B. Lendl, 3D Printing for low-cost and versatile attenuated  
599 total reflection infrared spectroscopy, *Anal. Chem.* 92 (2020) 4736–4741,  
600 <https://doi.org/10.1021/acs.analchem.9b04043>.

601 [29] A. Ambrosi, M. Pumera, 3D-printing technologies for electrochemical applications, *Chem.*  
602 *Soc. Rev.* 45 (2016) 2740–2755, <https://doi.org/10.1039/C5CS00714C>.

603 [30] G.D. da Silveira, R.F. Quero, L.P. Bressan, J.A. Bonacin, D.P. de Jesus, J.A.F. da Silva,  
604 Ready-to-use 3D-printed electrochemical cell for in situ voltammetry of immobilized  
605 microparticles and Raman spectroscopy, *Anal. Chim. Acta.* 1141 (2021) 57–62,  
606 <https://doi.org/10.1016/j.aca.2020.10.023>.

607 [31] P. Zambiasi, A. de Moraes, R. Kogachi, G. Aparecido, A. Formiga, J. Bonacin,  
608 Performance of water oxidation by 3D printed electrodes modified by prussian blue analogues,  
609 *J. Braz. Chem Soc* (2020), <https://doi.org/10.21577/0103-5053.20200088>.

610 [32] J.S. Stefano, C. Kalinke, R.G. da Rocha, D.P. Rocha, V.A.O.P. da Silva, J.A. Bonacin, L.  
611 Angnes, E.M. Richter, B.C. Janegitz, R.A.A. Munoz, ~ Electrochemical (Bio)sensors enabled  
612 by fused deposition modeling-based 3D printing: a guide to selecting designs, printing  
613 parameters, and post-treatment protocols, *Anal. Chem.* 94 (2022) 6417–6429,  
614 <https://doi.org/10.1021/acs.analchem.1c05523>.

615 [33] H. Agrawaal, J.E. Thompson, Additive manufacturing (3D printing) for analytical  
616 chemistry, *Talanta Open* 3 (2021), 100036, <https://doi.org/10.1016/j.talo.2021.100036>.

617 [34] J.M. Brisendine, A.C. Mutter, J.F. Cerda, R.L. Koder, A three-dimensional printed cell for  
618 rapid, low-volume spectroelectrochemistry, *Anal. Biochem.* 439 (2013) 1–3,  
619 <https://doi.org/10.1016/j.ab.2013.03.036>.

620 [35] M.D. Symes, P.J. Kitson, J. Yan, C.J. Richmond, G.J.T. Cooper, R.W. Bowman, T.  
621 Vilbrandt, L. Cronin, Integrated 3D-printed reactionware for chemical synthesis and analysis,  
622 *Nature Chem.* 4 (2012) 349–354, <https://doi.org/10.1038/nchem.1313>.

623 [36] E. Vaněčková, M. Bouřsa, F. Vivaldi, M. G' al, J. Rathouský, V. Kolivořska, T.  
624 Sebechlebská, UV/VIS spectroelectrochemistry with 3D printed electrodes, *J. Electroanal.*  
625 *Chem.* 857 (2020), 113760, <https://doi.org/10.1016/j.jelechem.2019.113760>.

626 [37] D.M. Wirth, M.J. Sheaff, J.V. Waldman, M.P. Symcox, H.D. Whitehead, J.D. Sharp, J.R.  
627 Doerfler, A.A. Lamar, G. LeBlanc, Electrolysis activation of fused-filamentfabrication 3D-

628 printed electrodes for electrochemical and spectroelectrochemical analysis, *Anal. Chem.* 91  
629 (2019) 5553–5557, <https://doi.org/10.1021/acs.analchem.9b01331>.

630 [38] J.H. da Silva Junior, J.V. de Melo, P.S. Castro, Lab-made 3D-printed accessories for  
631 spectroscopy and spectroelectrochemistry: a proof of concept to investigate dynamic interfacial  
632 and surface phenomena, *Microchim. Acta.* 188 (2021) 394, [https://doi.org/10.1007/s00604-](https://doi.org/10.1007/s00604-021-05041-3)  
633 021-05041-3.

634 [39] Y. Liu, M. Xia, L. Yao, M. Mensi, D. Ren, M. Gratzel, K. Sivula, N. Guijarro,  
635 Spectroelectrochemical and chemical evidence of surface passivation at zinc ferrite (ZnFe<sub>2</sub>O<sub>4</sub>)  
636 photoanodes for solar water oxidation, *Adv. Funct. Mater.* 31 (2021) 2010081,  
637 <https://doi.org/10.1002/adfm.202010081>.

638 [40] A. Ambrosi, R.R.S. Shi, R.D. Webster, 3D-printing for electrolytic processes and  
639 electrochemical flow systems, *J. Mater. Chem. A.* 8 (2020) 21902–21929, [https://](https://doi.org/10.1039/D0TA07939A)  
640 [doi.org/10.1039/D0TA07939A](https://doi.org/10.1039/D0TA07939A).

641 [41] O. Al'evêque, C. Gautier, E. Levillain, Real-time absorption spectroelectrochemistry:  
642 from solution to monolayer, *Curr. Opin. Electrochem.* 15 (2019) 34–41,  
643 <https://doi.org/10.1016/j.coelec.2019.03.015>.

644 [42] Y. Liu, F. Le Formal, F. Boudoire, N. Guijarro, Hematite photoanodes for solar water  
645 splitting: a detailed spectroelectrochemical analysis on the pH-dependent performance, *ACS*  
646 *Appl. Energy Mater.* 2 (2019) 6825–6833, <https://doi.org/10.1021/acsaem.9b01261>.

647 [43] E. Achilli, A. Minguzzi, A. Visibile, C. Locatelli, A. Vertova, A. Naldoni, S. Rondinini,  
648 F. Auricchio, S. Marconi, M. Fracchia, P. Ghigna, 3D-printed photospectroelectrochemical  
649 devices for in situ and in operando X-ray absorption spectroscopy investigation, *J. Synchrotron*  
650 *Radiat.* 23 (2016) 622–628, <https://doi.org/10.1107/S1600577515024480>.

651 [44] S.P. Best, V.A. Streltsov, C.T. Chantler, W. Li, P.A. Ash, S. Hayama, S. Diaz-Moreno,  
652 Redox state and photoreduction control using X-ray spectroelectrochemical techniques –  
653 advances in design and fabrication through additive engineering, *J. Synchrotron Radiat.* 28  
654 (2021) 472–479, <https://doi.org/10.1107/S1600577520016021>.

655 [45] K. Cheaib, B. Maurice, T. Mateo, Z. Halime, B. Lassalle-Kaiser, Time-resolved X-ray  
656 absorption spectroelectrochemistry of redox active species in solution, *J. Synchrotron Radiat.*  
657 26 (2019) 1980–1985, <https://doi.org/10.1107/S1600577519013614>.